RSC Advances

ROYAL SOCIETY OF CHEMISTRY

www.rsc.org/advances

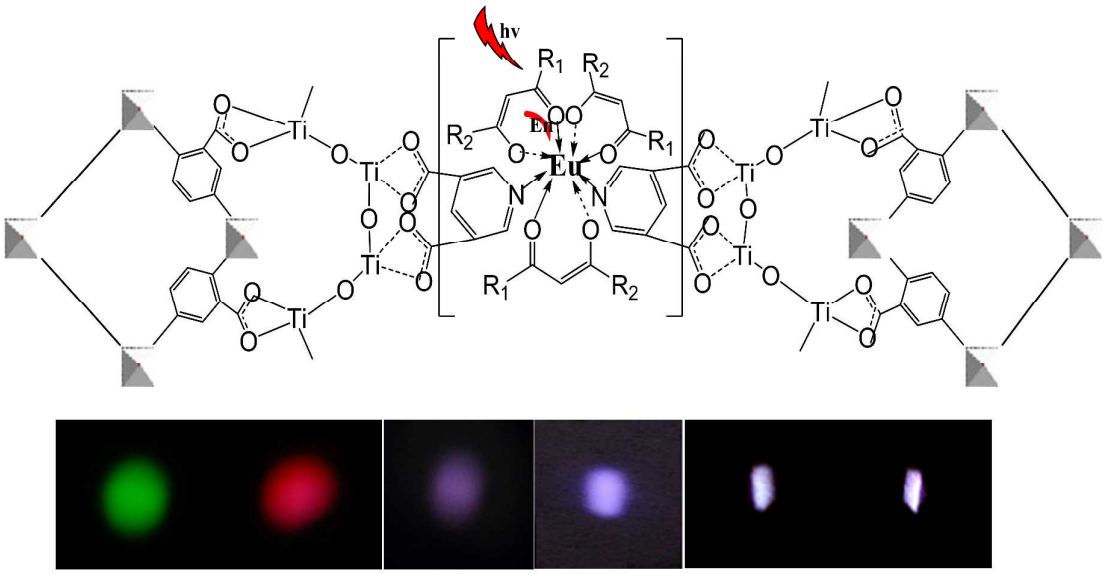

Multi-component sol-gel derived alumina and titania hybrid materials are assembled by the functionalization of both lanthanide complexes and special metal organic framework compound Al-MIL-53-COOH through coordination bonds. Multi-color luminescence and especially white color light can be tuned by controlling the different units in the hybrid system. In addition, the luminescent films are further prepared.

Journal Name

RSCPublishing

ARTICLE

Novel photofunctional hybrid materials (alumina and titania) functionalized with both MOF and lanthanide complexes through coordination bonds

Cite this: DOI: 10.1039/x0xx00000x

Received 00th January 2012,
Accepted 00th January 2012

DOI: 10.1039/x0xx00000x

www.rsc.org/

X. Y. Xu, B. Yan*

In the context, series of luminescent hybrid materials (alumina, titania) functionalized with both lanthanide complexes and metal organic frameworks (MOF, Al-MIL-53-COOH) through coordination bonds. In these hybrid systems, both MOF and lanthanide (Eu^{3+}, Tb^{3+}) complexes with beta-diketonates (2-thenoyltrifluoroacetonate (TTA), 1,1,1-trifluoroacetylacetonate (TAA), 2,4-pentanedionate (AA)) and pyridline-3,5-dicarboxylic acid (PDA) are coordinated to alumina and titania through their carboxylic groups. Al-MIL-53-COOH possesses the active –COOH group and can be linked to metallic alkoxides ($Ti[OCH(CH_3)_2]_4$, $Al[OCH(CH_3)_2]_3$) by post-synthesis path. Ternary complexes of beta-diketonates and PDA can be further bonded with metallic alkoxides through PDA as bridge for its coordinated carboxylic groups. After hydrolysis and condensation process, the final multi-component hybrid materials can be assembled and characterized. The photophysical properties of these hybrid materials are studied in detail, whose luminescent colour can be tuned by controlling the composition of different units in the hybrid system. Especially for the hybrids of europium complexes and MOF, the white luminescence can be obtained by integrating the emission of both europium complex and MOF. Furtherly, the luminescent films are prepared, which shows the uniformity and transparency. These results provide some useful data for the multi-component assembly and luminescent integration of photofunctional hybrid materials based with MOF and lanthanide units, which can be expected to have some potential application in luminescent devices for display or lighting.

Introduction

Photofunctional hybrid materials of both organic and inorganic networks provide a lot of opportunities to exhibit their extraordinary properties,[1] which are favorable for some potential applications in the practical fields such as lighting and displays, optical amplifiers, lasers fiber and photophysical sensing, *etc*.[2] Among which luminescent lanthanide hybrid systems are one of the fascinating fields, which keep generally luminescent character of lanthanide complexes, such as narrow and intense emission lines in visible and near infrared (NIR) region upon ultraviolet-visible light irradiation via effective intramolecular energy transfer process. [3] In the recent years, considerable researches are carried out on versatile lanthanide hybrid materials and some universal strategies or paths to achieve special chemical linkers to construct hybrid systems [4-6]. Among which it is worthy pointing out that the most predominant topic is focused on the organically modified silica derived hybrid materials,[5,6] whose sol-gel technology make it become practical to fabricate all kinds of active units in the construction of hybrids. Subsequently, the thermal stabilities and photophysical properties of lanthanide complexes can be improved.[7,8] Furtherly, polymer units can be introduced into lanthanide hybrid system and is of significance for the potential application in optical devices.[9,10]

Moreover, the amorphous organically modified silica network hybrids can be transferred to ordered mesoporous silica with special surfactants or other templates, whose regular pore structure, high photostability and thermal stability are suitable host for guest-host assembly chemistry of photoactive species. Nowadays, lanthanide hybrids based with functionalized mesoporous host have been prepared, involving MCM-41(48), SBA-15(16) and POMs, *etc*.[11-13] The highly ordered structures and uniform tunable pore sizes will expand the applications of these photofunctional hybrids in optical or electronic areas.

But the above silica-derived hybrid materials including mesoporous hybrids are mainly belong to the amorphous state materials, whose non-crystalline nature make them very difficult to exactly study the composition and structure in the hybrid system. In order to ameliorate this problem, one effort is to introduce crystalline unit in the hybrid system to keep the exact coordination environment around lanthanide ions, such as lanthanide polyometallates as the central species.[14,15] More extensive strategy is to functionalize the crystalline host, such as traditional microporous zeolite, and some host-guest hybrid materials based with zeolite are developed.[16] Metal organic frameworks (MOF) are crystalline materials with regular porous networks constructed from organic linker molecules and

metal ions.[17] Luminescent MOFs possess high, well-defined porosity and intense fluorescence, which gathers considerable attention owing to their potential applications in chemical sensors, light emitting devices and biomedicine.[18] The abundant groups in MOFs make it possible to be modified by the so-called post-synthesis strategy.[19] This provides great potential to construct hybrid system based on MOFs.

Al-MIL-53-COOH is a high crystalline framework that consists of regular one-dimensional channels (Figure S1 in ESI), which shows high structural flexibility.[20] The presence of non-coordinating carboxyl group, as well as the high thermal and chemical stabilities makes it a good candidate to assemble hybrid materials with other photoactive units. So in this paper, we fabricate Al-MIL-53-COOH and lanthanide complexes in inorganic matrices (alumina or titania) through coordination bonds to assemble the multi-component hybrid materials, whose physical characterization and luminescent properties are studied in detail.

EXPERIMENT SECTION

Starting materials

Al-MIL-53-COOH (MOF) nanoparticles were synthesized according to the synthesis method and conditions (molar ratio, time and temperature) described in the literature [20] using $AlCl_3{\cdot}6H_2O$ and trimellitic acid (1, 2, 4-benzenetricarboxylic acid). Two lanthanide chloride $LnCl_3{\cdot}xH_2O$ (Ln = Eu, Tb) were prepared by dissolving their oxides (Eu_2O_3, Tb_4O_7) into the concentrated hydrochloric acid (37 %) with heating and stirring to promote the reaction until that the crystal film appeared. 2-Thenoyltrifluoroacetone (99 %, TTA, Adamas), 1,1,1-trifluoroacetylacetone (98 %, TAA, Adamas), 2,4-pentanedione (99 %, AA, Adamas), aluminum isopropoxide (99 %, Adamas) tetraisopropoxytitanium (98 %, Adamas) and pyridline-3,5-dicarboxylic acid (98 %, PDA, Adamas) were used as received. All the other reagents are analytical pure and used without purification.

Synthesis of nanosized MOF (Al-MIL53-COOH) and MOF-Al/Ti precursors

Al-MIL-53-COOH nanoparticles were synthesized by solvothermal method [20] using aluminum chloride $AlCl_3{\cdot}6H_2O$, trimellitic acid (H_2BDC-COOH) and N,N-dimethylformamide (DMF). The following optimal reaction conditions were extracted: (1) the molar ratio of Al^{3+}: H_2BDC–COOH is 1: 1; (2) the temperature was kept as 180 °C for 12 hrs. The reactants were stirred a few minutes before transferring the resulting suspension to a Teflon-lined steel autoclave. The resulting nanocrystals were separated by centrifugation at 16000 rpm for 10 min, then washed three times with ethanol to remove the excess of unreacted aluminum chloride species and trimellitic acid and dried at 200 °C for 6 hrs to remove the adsorbed DMF molecules. Whose scheme for its crystal structure and the XRD pattern has been shown in Figures S1 and S2 in ESI. The MOF-Al/Ti precursors were prepared by mixing MOF and $Al[OCH(CH_3)_2]_3$ (or $Ti[OCH(CH_3)_2]_4$) with molar ratio 1: 2 after refluxing at 70 °C for 6 hrs.

Synthesis of lanthanide hybrid hydrogels

Preparation of L-Ln-PDA-Al/Ti system (Ln = Eu, L = TTA, TAA; Ln = Tb, L = TAA, AA) In this step, we prepared eight species of lanthanide hybrid hydrogels. Here we took the synthesis of TTA-Eu-PDA-Ti as an example: 1) 3 mmol TTA were dissolved in appropriate amount of anhydrous ethanol using 3 mmol NaOH to destroy molecular structure of the methylene proton in the reaction system. The solution was kept at 60 °C for 2 hrs and then 1 mmol $EuCl_3{\cdot}6H_2O$ was dropped in above solution. The mixture solution was continued at 60 °C for 1 hr and then cooled, filtered to remove the white precipitate NaCl to obtain the resulting product Eu-TTA: 2) 2 mmol PDA were dispersed in the ethanol firstly and then appropriate amount of aluminum isopropoxide (Eu^{3+}: $Al[OCH(CH_3)_2]_3$ = 1: 20) were added. After stirring for a while, NH_4OH was added and whole solution was under refluxing at 70 °C for 6 hrs in oil bath. The two above solutions are mixed together, and then the mixture solution of Eu-TTA-Ti was formed.

Preparation of L-Ln-PDA-Al/Ti-MOF hybrid system (Ln = Eu, L = TTA, TAA; Ln = Tb, L = TAA, AA) Mixing the solutions of MOF-Al/Ti and L-Ln-PDA-Al/Ti with molar ratio of 10: 1 and then 160 mmol deionized water were dropped into the above solution to promote the hydrolysis of $Al[OCH(CH_3)_2]_3$ ($Ti[OCH(CH_3)_2]_4$) and the formation of hydrogel was constructed by Al-O or Ti-O network. Then the final material L-Ln-PDA-Al/Ti-MOF was obtained after centrifuge and washed with ethanol for three times and dried at 60 °C. The contents of metal ions (Eu^{3+}, Tb^{3+}, Al^{3+}, Ti^{4+}) and N in the hybrids were determined. It is hardly to determine the exact composition of them within the complicated hybrid system, but we can predict the ratio among different units based with their contents in the whole hybrid materials. For TTA-Eu-PDA-Al-MOF: Eu 2.49 %, Al 21.30 %, N 0.43 %; for TAA-Eu-PDA-Al-MOF: Eu 2.58 %, Al 22.05 %, N 0.45 %; for TAA-Tb-PDA-Al-MOF: Tb 2.61 %, Al 22.00 %, N 0.44 %; for AA-Tb-PDA-Al-MOF: Tb 2.77 %, Al 22.81%, N 0.48 %; for TTA-Eu-PDA-Ti-MOF: Eu 2.11 %, Al 3.65 %, Ti 26.82 %, N 0.38 %; for TAA-Eu-PDA-Ti-MOF: Eu 2.19 %, Al 3.74 %, Ti 27.60 %, N 0.40 %; for TAA-Tb-PDA-Ti-MOF: Tb 2.29 %, Al 3.75 %, Ti 27.64 %, N 0.39 %; for AA-Tb-PDA-Ti-MOF: Tb 2.33 %, Al 3.82 %, Ti 28.20 %, N 0.40 %. According to the content of Ln^{3+} and N, it can be predicted the molar ratio of Ln: N is close to 1: 2, suggesting the two PDA ligands coordinated to Ln^{3+}. Besides, for alumina, the molar ratio of Ln^{3+}: Al^{3+} is close to 1: 50, while for titania, the molar ratio of Ln^{3+}: Al^{3+}: Ti^{4+} is close to 1: 10: 40, both of which take agreement with the reaction molar ratio. Therefore, the above preparation reaction can be controlled, and the scheme in Figure 1 is acceptable for the composition of these hybrid systems.

Preparation of thin films of lanthanide hybrid hydrogels (TTA/TAA-Eu-PDA-Ti-MOF)

The lanthanide hybrid hydrogel thin films of Al-MIL-53-COOH assemblies were prepared by direct dip-coating their colloidal solution at room temperature and under ambient pressure, using a pre-cleaned 1 cm × 1 cm ITO glass which was fixed on a Laurell spin-coater. The spin rate and spin time were kept at 1000 rpm for 60 s. The solvent adsorbed was removed by drying the thin films at room temperature after spin-coating.

Physical characterization

Fourier transform infrared (FTIR) spectra were measured within the 4000-400 cm^{-1} region on the infrared spectrophotometer with the KBr pellet technique. The contents of Eu^{3+}, Tb^{3+}, Al^{3+} and Ti^{4+} in the hybrids were determined with Inductively Coupled Plasma Optical

Emission Spectrometer (ICP-OES). The elemental analyses of nitrogen element are measured with a CARIO-ERBA 1106 elemental analyser. The room temperature X-ray powder diffraction patterns (XRD) were recorded on a Rigaku D/max-rB diffractometer equipped with a Cu anode in a 2θ range from 10-70 °. The scanning electronic microscope (SEM) images were obtained with a Philips XL-30. Nitrogen adsorption/desorption isotherms were measured at the liquid nitrogen temperature, using a Nova 1000 analyzer. Surface areas were calculated by the Brunauer–Emmett–Teller (BET) method. The luminescent spectra were measured on an Edinburgh FLS920 phosphorimeter using a 450 W xenon lamp as excitation source. The outer luminescent quantum efficiency was measured using an integrating sphere (150 mm diameter, $BaSO_4$ coating) with the Edinburgh FLS920 phosphorimeter. The luminescence spectra were corrected for variations in the output of the excitation source and for variations in the detector response. The quantum yield was defined as the integrated intensity of the luminescence signal.

Results and discussion

The scheme for the synthesis process, composition and proposed structure of TTA/TAA-Eu-PDA-Ti-MOF is shown in Figure 1. Metallic alkoxides ($Ti[OCH(CH_3)_2]_4$, $Al[OCH(CH_3)_2]_3$) can be modified by carboxylic group reagents such as PDA, which has been proved by many previous works [21]. Then the lanthanide beta-diketonates can further coordinate to PDA modified metallic alkoxides for the high coordination number and remained nitrogen atom of PDA, resulting in the eight coordinated complexes.[21,22] On the other hand, Al-MIL-53-COOH (MOF) can be also introduced in the courses of sol-gel reaction process to form alumina and titania for its uncoordinated COOH group. Subsequently, after the hydrolysis and polycondensation process of metallic alkoxides, the final hybrid materials based with alumina or titania are prepared and the photoactive units of MOF and lanthanide complexes are chemically linked. Here we only set up Eu-TTA/TAA-Ti-1 as an example; other hybrids show the similar scheme except for different beta-diketonates or alumina.

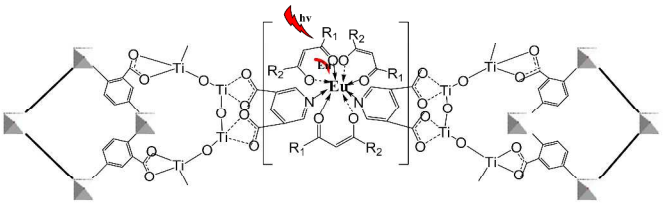

Figure 1 The selected scheme for the synthesis process, composition and proposed structure of TTA/TAA-Eu-PDA-Ti-MOF, other hybrid systems show the similar scheme except for different beta-diketonates or alumina unit.

Figure 2a depicts the FTIR spectrum of compound MOF. The 3454 cm^{-1} at high frequency region is corresponding to the adsorbed water molecules. The absorption peaks at 1675 cm^{-1} (ν_{as}) and 1453, 1419 cm^{-1} (ν_s) suggests the presence of the carboxylic acids and carboxylate. The absorption peaks at 1170 and 785 cm^{-1} are ascribed to the C-H deformation vibrations of the aromatic ring. Figure 2b shows the selected FT-IR spectra of the final hybrids Eu-TTA/TAA-Ti/Al-MOF. The characteristic stretching vibrations of the coordinating carboxylate groups are easily visible, ν_{as} at 1613 and ν_s at 1402 or 1379 cm^{-1}, revealing that the further coordination to Ti or Al in the hybrids produces the red-shift of frequency of COO^- group in MOF. The presence of water molecules can be evidenced by the band with a broad band in high frequency region over 3200 cm^{-1}. Besides, it is worthy pointing out that the more absorption bands of the functional groups in organic ligands (TTA, TAA) cannot be checked clearly for their limited amount in the whole hybrid system.

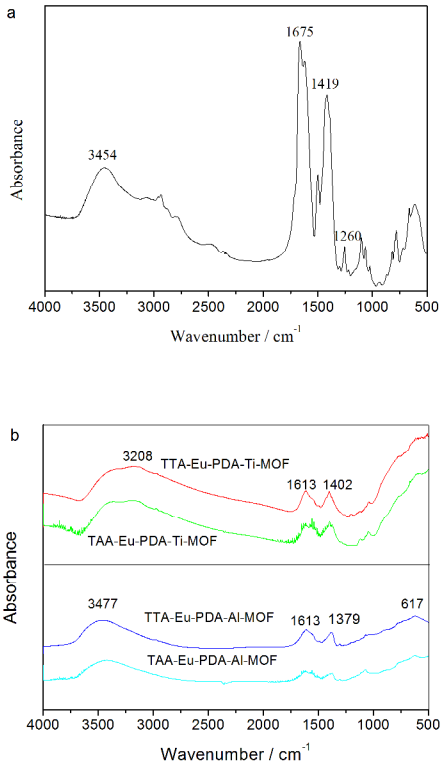

Figure 2 The Fourier transform infrared spectra of Al-MIL-53-COOH (MOF) (a) and selected hybrid materials (b).

Figure 3 shows the selected SEM images of the hybrids TAA-Tb-PDA-Al-MOF (a) and TTA-Eu-PDA-Ti-MOF (b), respectively. Both of them show little distinction between their morphology. Compared the bulk Tb-TAA-Al-MOF hybrids, Eu-TTA-Ti-MOF shows more soft and fine microstructure. This may be related to the different sol-gel reaction behaviour of Al and Ti precursors.

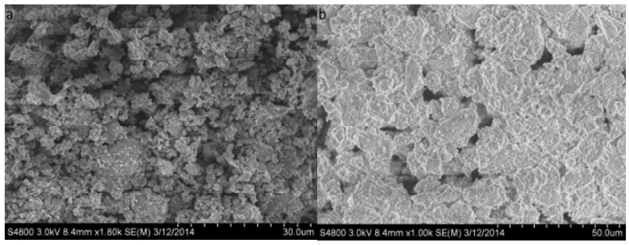

Figure 3 The selected SEM images of hybrid materials TAA-Tb-PDA-Al-MOF (a) and TTA-Eu-PDA-Ti-MOF (b)

Figure S3 shows the X-ray diffraction patterns (from 10 to 70 °) of hybrid materials L-Eu/Tb-PDA-Al/Ti-MOF (a) alumina system and (b) titania system (Eu^{3+}, L = TTA, TAA; Tb^{3+}, L = TAA, AA). Both of alumina and titania hybrids present the dominant broad band, belonging to the amorphous state of alumina or titania gels (Al-O network and Ti-O network). For the limited fabrication amount of MOF in the hybrids, the crystalline diffraction peaks for MOF cannot be identified clearly in these XRD patterns. Comparing with the two figures, Eu-TTA/TAA-Al-MOF hybrids seem to show slightly better crystallization than Eu-TTA/TAA-Ti-MOF systems, well consistent with the SEM of the product obtained. Considering the same Al^{3+} ion component in both MOF and alumina, the corresponding crystalline state may be good. It needs to be clarified that in the hybrid system, the host is titania or alumina and lanthanide complex or MOF are all active unit in the titania or alumina host. So MOF and lanthanide complex both possess small amount in the large amount of host titania or alumina. So the final PXRD patterns present the main feature of host titania or alumina and it is hardly to check the character of lanthanide complex or MOF. Naturally, the crystalline character of MOF is impossible to be shown clearly from the PXRD pattern. In addition, for the above-mentioned reason, the structure of TTA-Eu-PDA-Ti@MOF and TTA-Tb-PDA-Ti@MOF, TAA-Tb-PDA-Al@MOF and TAA-Eu-PDA-Al@MOF from XRD should mainly show the character of amorphous titania for TTA-Eu-PDA-Ti@MOF and TTA-Tb-PDA-Ti@MOF and alumina for TAA-Tb-PDA-Al@MOF and TAA-Eu-PDA-Al@MOF, respectively, while not MOF for its limited content.

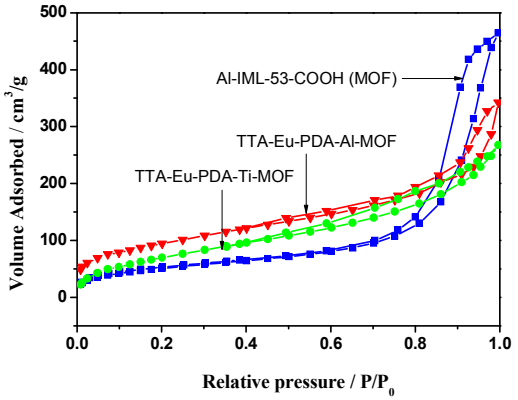

Figure 4 N_2 adsorption-desorption isotherms of compound Al-MIL-53-COOH (MOF) and TTA-Eu-PDA-Al/Ti-MOF.

Figure 4 presents the N_2 adsorption-desorption isotherms of compound Al-MIL-53-COOH (MOF) and TTA-Eu-PDA-Al/Ti-MOF hybrids. It indicates that the final hybrid material can show porosity toward N_2. Unlike other microporous materials, both belong to type I adsorption curve, these samples display typical type IV curves with hysteresis loops at high relative pressure. The steric hindrance of the free non-coordinated carboxyl groups in the channels of MOF leads to the atypical hysteresis of the N_2 adsorption isotherms, which reduces the access of N_2 molecules. TTA-Eu-PDA-Al/Ti-MOF samples exhibit similar sorption behavior with MOF. The BET surface area of Al-MIL-53-COOH(MOF) is 394 m^2g^{-1}. While the hybrids TTA-Eu-PDA-Al/Ti-MOF samples exhibit similar sorption behavior with Al-MIL-53-COOH (MOF). The BET surface areas of TTA-Eu-PDA-Al-MOF and TTA-Eu-PDA-Ti-MOF are 345 m^2g^{-1} and 339 m^2g^{-1}, respectively, which show reasonable reduction in comparison with the surface area of Al-MIL-53-COOH (MOF) may be due to the uploading of some small molecules exist in the hybrid alumina or titania host. MOF is fabricated in alumina or titania host can easily to be affected by other components within the host.

The excitation and emission spectrum and the CIE chromaticity diagram of MOF (Al-MIL-53-COOH) are shown in Figure S4. The maximum excitation and emission wavelength are 372 nm and 420 nm, respectively. This can be ascribed as the excitation and emission of trimellitic acid ligand. The corresponding CIE chromatic coordinate of MOF is located in the light blue region, which can be composed with the luminescent species in yellow-orange-red region to white emission. This predicts can be proved from the following hybrids fabricated Eu^{3+} complexes.

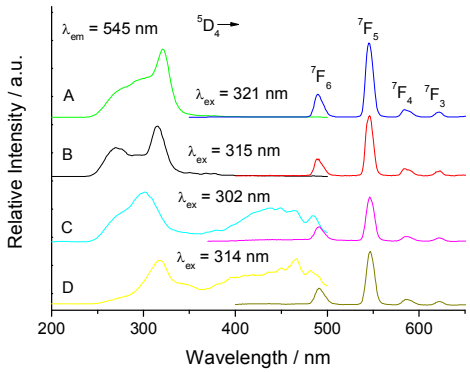

Figure 5 The excitation and emission spectra of terbium hybrid materials TAA-Tb-PDA-Al-MOF (A), AA-Tb-PDA-Al-MOF (B), TAA-Tb-PDA-Ti--MOF (C) and AA-Tb-PDA-Ti-MOF (D)

Figure 5 shows the luminescent excitation and emission spectra of Tb hybrids TAA-Tb-PDA-Al-MOF (A), AA-Tb-PDA-Al-MOF (B), TAA-Tb-PDA-Ti--MOF (C) and AA-Tb-PDA-Ti-MOF (D). Their excitation bands are similar with wide range of 250 ~ 350 nm, corresponding to the excitation of beta-diketonates and carboxylic acid unit of MOF. No excitation peaks to the f-f transitions of Tb^{3+} can be checked. In titania hybrid system, the above excitation bands become narrow and another wide excitation in visible region can be observed. This may be due to the titania is not so favourable as alumina for luminescence of Tb^{3+} complexes, which is found in many previous studies.[20] Organic ligands absorb the energy and then transfer it to the accepting energy level of lanthanide ions. The wide excitation bands are favourable for the energy transfer and luminescence of Tb^{3+}. The corresponding emission spectra of all terbium hybrids present the characteristic luminescence of Tb^{3+}, while no emission of MOF could be checked. The emission lines are assigned to the $^5D_4 \rightarrow {}^7F_J$ transitions of Tb^{3+}, locating at around 490, 545, 587 and 623 nm, for J = 6, 5, 4 and 3, respectively. The most striking green luminescence is for $^5D_4 \rightarrow {}^7F_5$ transition. Besides, it can be seen that no excitation and emission bands for MOF can be checked, suggesting that there are no overlap and energy transfer between the MOF and terbium complexes.

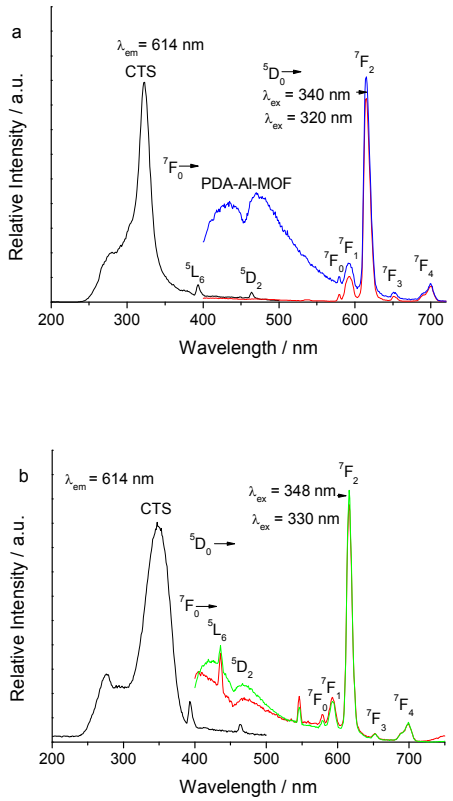

Figure 6 The excitation and emission spectra of the hybrids TAA-Eu-PDA-Al-MOF (a) and TTA-Eu-PDA-Al-MOF (b).

Figure 6 shows the luminescent excitation and emission spectra of hybrids TAA-Eu-PDA-Al-MOF (a) and TTA-Eu-PDA-Al-MOF (b), respectively. Different from the above terbium hybrids, the excitation spectra by monitoring the emission of Eu^{3+} at 614 nm show both excitation of organic ligands and f-f transition of Eu^{3+}. A broad excitation band from 250 to 380 nm centered at about 320 nm (TAA-Eu-PDA-Al-MOF) and 340 nm (TTA-Eu-PDA-Al-MOF) in the ultraviolet region, which is attributed to the absorption from the organic ligands to form the charge transfer state (CTS) of Eu-O. The shoulder excitation bands at low wavelength of 270 or 280 nm suggest the excitation of TTA or TAA ligands. At the same time, there exist peaks at around 396 and 467 nm owing to the narrow f-f absorption transition ($^7F_0 \rightarrow {}^5L_6$ and $^7F_0 \rightarrow {}^5D_2$) of Eu^{3+} ion, whose intensity is much weaker than the absorption from organic ligands. The emission bands of the two hybrid materials are assigned to the $^5D_0 \rightarrow {}^7F_J$ (J = 0 - 4) transitions of Eu^{3+} at 580, 591, 614, 652, and 700 nm under two different kinds of excitation wavelengths (320/340 nm, 330/348 nm). It is noteworthy that different excitation wavelength may have influence on the emission spectra, which is shown apparently in Figure 6(a)). Under excitation of 340 nm, both emission of MOF and Eu-TAA complex can be observed and the different luminescence spectral position in the visible region may be expected to adjust the final luminescence color of the hybrids. This will be shown clearly in the following CIE diagraphs. While for the excitation of 320 nm, no apparent luminescence of MOF is observed but presents only the red emission of europium TAA complexes. From the result, it can be found that the excitation at 320 nm is mainly from the ligands of TTA to form CTS, while not for MOF. The absorption at 340 nm does not produce the strong emission of Eu^{3+} and it is overlap with the excitation of MOF in Figure S4. So the emission of MOF can be observed. For TTA-Eu-PDA-Al-MOF hybrids, no distinction appears for the two different excitation wavelengths, whose two emissions of MOF and Eu-TTA are both observed.

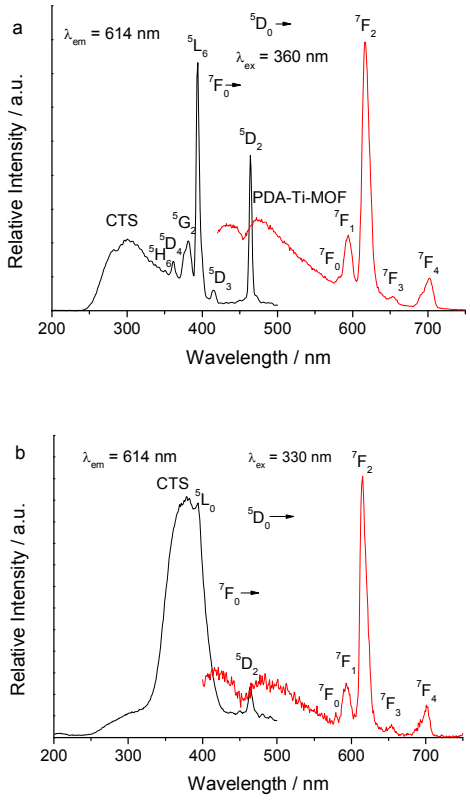

Figure 7 The excitation and emission spectra of hybrid materials TTA-Eu-PDA-Ti-MOF (a) and TAA-Eu-PDA-Ti-MOF (b).

The luminescent spectra of titania hybrids are shown in Figure 7. The excitation spectra by monitoring the emission of Eu^{3+} at 614 nm of europium hybrids show both excitation of organic ligands and f-f transition of Eu^{3+}, which presents the apparent distinction. For Eu-TAA-Ti-MOF hybrids, its excitation spectrum consists of a broad excitation ultraviolet band from 250 to 350 nm centered at about 300 nm and series of sharp excitation peaks covering 350 to 500 nm in the ultraviolet-visible region. The former is ascribed as the absorption from the organic ligands to form the charge transfer state (CTS) of Eu-O. The latter belongs to the f-f absorption transition (327 nm, $^7F_0 \rightarrow {}^5H_6$; 363 nm, $^7F_0 \rightarrow {}^5D_4$; 383 nm, $^7F_0 \rightarrow {}^5G_2$; 394 nm, $^7F_0 \rightarrow {}^5L_6$, strongest; 415 nm, $^7F_0 \rightarrow {}^5D_3$; 467 nm, $^7F_0 \rightarrow {}^5D_2$) of Eu^{3+} ion.[23] It is worthy point out that the intensity of them is strong, even stronger than the absorption from organic ligands. While for Eu-TTA-Ti-MOF hybrids, the CTS excitation from organic ligand is much stronger than the f-f transition so that only two narrow f-f absorption transition ($^7F_0 \rightarrow {}^5L_6$, 396 nm and $^7F_0 \rightarrow {}^5D_2$, 466 nm) of Eu^{3+} ion can be checked. The excitation at 396 nm appears as a shoulder peak in the broad excitation bands of CTS (300-450 nm

rang centered 370 nm). Both of the two hybrids show the similar shape of emission spectra consisting of Eu^{3+} ion and MOF. The emission to the $^5D_0 \rightarrow {}^7F_J$ (J = 0 - 4) transitions of Eu^{3+} is located at 580, 591, 614, 652, and 700 nm. The appearance of wide emission of MOF at 400 to 580 nm may be expected to integrate with the emission of Eu^{3+}, which is shown in the following CIE diagrams.

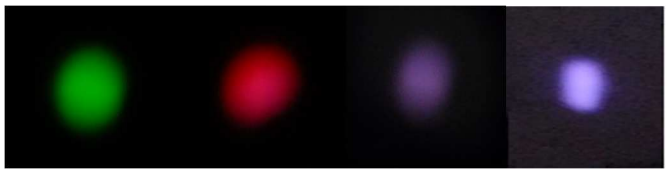

Figure 8 Photographs of the photoluminescence colour from power with the UV excitation using a Xe lamp as the excitation source. The images from left to right stand for hybrid materials TAA-Tb-PDA-Al-MOF, TAA-Eu-PDA-Al-MOF, TTA-Eu-PDA-Al-MOF and TAA-Eu-PDA-Ti-MOF, respectively.

Figure 8 gives the selected photographs of four hybrid materials TAA-Tb-PDA-Al-MOF, TAA-Eu-PDA-Al-MOF, TTA-Eu-PDA-Al-MOF and TAA-Eu-PDA-Ti-MOF, respectively. Among which three hybrids based with alumina, TAA-Tb-PDA-Al-MOF and TAA-Eu-PDA-Al-MOF hybrids show the typical bright green for Tb^{3+} and red emission for Eu^{3+}; while Eu-TTA-Al-MOF hybrids present pink-white colour emission. For Eu-TAA-Ti-MOF hybrids, it presents the close white luminescence. So these hybrids can realize the multi-colour light output by adjusting the component and excitation wavelengths.

Figure S5 shows the CIE diagrams of the spectra in Figures 6 and 7, TAA-Eu-PDA-Al-MOF (a), TTA-Eu-PDA-Al-MOF (b), TTA-Eu-PDA-Ti-MOF (c) and TAA-Eu-PDA-Ti-MOF (d), respectively. From these four diagrams, it can be found that the selectively excitation with suitable wavelength can realize the output of close white luminescence. For TAA-Eu-PDA-Al-MOF hybrids, the white colour luminescence can be obtained using λ_{ex} of 320 nm, while the blue-white emission using λ_{ex} of 340 nm. For TTA-Eu-PDA-Al-MOF hybrids, the two excitation wavelengths show the CIE coordinates in close white (330 nm) and pink-white (348 nm) region. For the two kinds of hybrid materials based with titania (TTA-Eu-PDA-Ti-MOF, TAA-Eu-PDA-Ti-MOF), they both show the typical white luminescence. The parent MOF and other hybrid systems present blue and green color emission, respectively, whose CIE diagrams of spectra are shown in Figure S6. The detailed CIE coordinates are summarized in Table 1.

Table 1 The luminescence data of MOF and the lanthanide hybrid materials

Materials	λ_{em} (nm)	λ_{ex} (nm)	Colour (CIE-X,Y)	η (%)
Al-MIL-53-COOH (MOF)	420	372	Blue (0.1669,0.1398)	17.0
TTA-Eu-PDA-Al-MOF	614	330	Close white (0.3456,0.2604)	3.3
	614	348	Pink-white (0.3160,0.2261)	3.7
TAA-Eu-PDA-Al-MOF	614	320	White (0.3602,0.3186)	11.1
	614	340	Blue-white (0.2692,0.2379)	13.2
TAA-Tb-PDA-Al-MOF	545	321	Green (0.2972,0.6030)	8.2
AA-Tb-PDA-Al-MOF	545	315	Green (0.3062,0.5984)	15.6
TTA-Eu-PDA-Ti-MOF	614	330	White (0.3525,0.2844)	0.9
TAA-Eu-PDA-Ti-MOF	614	360	White (0.3272,0.2804)	4.5
TAA-Tb-PDA-Ti-MOF	545	302	Green (0.2807,0.5061)	0.7
AA-Tb-PDA-Ti-MOF	545	314	Green (0.2901,0.5358)	0.4

Moreover, the absolute luminescence quantum yield data are obtained with an integrating sphere and a calibrated detector setup for solid materials. The resulting absolute luminescence quantum yields are listed in Table 1. The luminescent quantum yields of the hybrids based with alumina are higher than those with titania, which takes agreement with the results from other reported lanthanide hybrids functionalized alumina and titania.[21,22] Comparatively, alumina is more favourable for the luminescence of lanthanide species than tiania.[21,22] The rule of the η values of them are not apparent for the complicated hybrids system, TAA-Eu-PDA-Al-MOF hybrid material possess white colour luminescence and 11.1 % quantum efficiency (λ_{ex} = 320 nm), which is benefit for the further study. For comparison, we selectively measure the luminescent quantum yields of four lanthanide hybrid (alumina or titania) materials themselves without MOF: they are 21.4 % (TAA-Eu-PDA-Al), 6.2 % (TAA-Eu-PDA-Ti), 17.0 (TAA-Tb-PDA-Al) and 2.1 % (TAA-Tb-PDA-Ti), respectively. These values are all higher than those of hybrids with both lanthanide complexes and MOF, which is due to the much lower content of lanthanide complexes in the hybrids with MOF than those of hybrids without MOF.

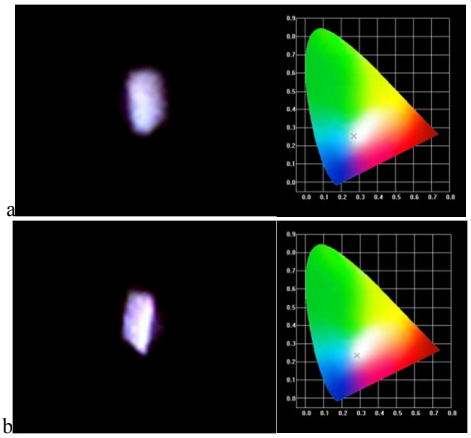

Figure 9 The photograph (left) and CIE chromaticity diagram (right) of the prepared thin film based with TTA-Eu-PDA-Ti-MOF (a, λ_{ex} = 330 nm) and TAA-Eu-PDA-Ti-MOF (b, λ_{ex} = 360 nm) hybrids.

Furtherly, we try to prepare the hydrogel thin films based with TTA-Eu-PDA-Ti-MOF (a, left) and TAA-Eu-PDA-Ti-MOF (b, right) hybrids, whose pictures are shown in Figure S7. Both of the two hybrid thin films are uniform and transparent, suggesting that it is feasible to prepare such hybrid thin film for further optical application. Figure S8 shows the excitation and emission spectra of hybrid thin films fabricated with TTA-Eu-PDA-Ti-MOF (a) and TAA-Eu-PDA-Ti-MOF (b), which presents the similar feature as the spectra of their powder samples. Their luminescent spectra consist of the emission from both europium beta-diketonates (TTA, TAA) and MOF functionalized titania host at red region and blue-green one, respectively, integrating the white colour luminescence. Figure 9(a) and (b) show the photograph and CIE diagrams of the two hybrid thin films.

Conclusions

In the context, multi-component sol-gel derived alumina and titania hybrid materials are assembled by the functionalization of both lanthanide complexes and special metal organic framework compound Al-MIL-53-COOH through coordination bonds. Al-MIL-53-COOH can be fabricated to alumina and titania through

postsynthesis for its free carboxylic groups. Lanthanide beta-diketonates can be introduced into alumina and titania with a special chemical linker pyridline-3,5-dicarboxylic acid. After hydrolysis and condensation process, the multi-component hybrid materials can be prepared. The multi-colour luminescence can be tuned by controlling the different units in the hybrid system. Among which white colour light input can be realized by integrating the emission of both europium complex and MOF. In addition, the luminescent uniform and transparent films are further prepared. These results provide some useful data for further practical application in photofunctional devices.

Acknowledgements

This work was supported by the National Natural Science Foundation of China (91122003) and Developing Science Funds of Tongji University.

Notes and references

[a] Department of Chemistry, Tongji University; State Key Lab of Water Pollution and Resource Reuse, Siping Road 1239, Shanghai 200092, China. Fax: +86-21-65981097; Tel: +86-21-65984663; E-mail: byan-tongji.edu.cn

† Electronic Supplementary Information (ESI) available: [details of any supplementary information available should be included here]. See DOI: 10.1039/b000000x/

1 (*a*) B. Lebeau and C. Sanchez, Current Opinion in Solid State and Materials, 1999, **4**, 11; (*b*) Pedro and C. Sanchez, *Functional hybrid materials*, WILEY-VCH Verlag GmbH & Co. KGaA, 2006; (*c*) T. Umeyama and H. Imahori, *J. Phys. Chem. C*, 2013, **117**, 3195.

2 (*a*) P. Innocenzi and B. Lebeau, *J. Mater. Chem.*, 2005,**15**, 3821; (*b*) B. Lebeau and P. Innocenzi, *Chem. Soc. Rev.*, 2011, **40**, 886; (*c*) L. D. Carlos, R. A. S. Ferreira, V. D. Bermudez, B. Julian-Lopez and P. Escribano, *Chem. Soc. Rev*., 2011, **40**, 536.

3 (*a*) L. N. Sun, H. J. Zhang, Q. G. Meng, F. Y. Liu, L. S. Fu, C. Y. Peng and J. B. Yu, *J. Phys. Chem. B*, 2005, 1**09**, 6174; (*b*) Y. J. Gu and B. Yan, *J. Coll. Interf. Sci.*, 2013, **393**, 36; (*c*) Y. J. Gu and B. Yan, *Eur. J. Inorg. Chem.*, 2013, 2963; (d) Y. Y. Li, B. Yan and X. F. Qiao, *Microp. Mesop. Mater.*, 2013, **169**, 60.

4 (*a*) L. D. Carlos, R. A. S. Ferreira, V. D. Bermudez and S. J. L. Ribeiro, *Adv. Mater.*, 2009, **21**, 509; (*b*) K. Binnemans, *Chem. Rev.*, 2009, **109**, 4283; (*c*) B. Yan, *RSC Adv.*, 2012, **2**, 9304; (*d*) J. Feng, H. J. Zhang, *Chem. Soc. Rev.*, 2013, **42**, 387.

5 (*a*) H. R. Li, J. B. Yu, F. Y. Liu, H. J. Zhang, L. S. Fu, Q. G. Meng, C. Y. Peng and J. Lin, *New J. Chem.*, 2004, **28**, 1137; (*b*) Q. M. Wang, and B. Yan, *J. Mater. Chem.*, 2004, **14**, 2450; (*c*) Q. M. Wang and B. Yan, *Cryst. Growth Des.*, 2005, **5**, 497; (*d*) L. Guo and B. Yan, *Eur. J. Inorg. Chem.*, 2010, 1267; (*e*) J. L. Liu and B. Yan, *Dalton Trans.*, 2011, **40**, 1961.

6 (*a*) A. C. Franville, D. Zambon and R. Mahiou, *Chem. Mater.*, 2000, **12**, 428; (*b*) H. F. Lu, B. Yan and J. L. Liu, *Inorg. Chem.*, 2009, **48**, 3966; (*c*) J. L. Liu, B. Yan and L. Guo, *Eur. J. Inorg. Chem.*, 2010, 2290; (*d*) B. Yan and H. F. Lu, *Inorg. Chem.*, 2008, **47**, 5601.

7 (*a*) M. Fernandes, V. D. Bermudez, R. A. S. Ferreira, L. D. Carlos, M. M. Silva and M. J. Smith, *Chem. Mater.*, 2007, **19**, 3892; (*b*) F. Y. Liu, L. D. Carlos, R. A. S. Ferreira, J. Rocha, M. C. Gaudino, M. Robitzer and F. Quignard, *Biomolecules*, 2008, **9**, 1945; (*c*) S. S. Nobre, C. D. S. Brites, R. A. S. Ferreira, V. D. Bermudez, C. Carcel, J. I. E. Moreau, J. Rocha, M. W. C. Man and L. D. Carlos, *J. Mater. Chem.*, 2008, **18**, 4172.

8 (*a*) H. F. Lu and B. Yan, *J. Non-Cryst. Solids*, 2006, **352**, 5331; (*b*) B. Yan and Q. M. Wang, *Cryst. Growth Des.*, 2008, **8**, 1484; (*c*) L. Guo, B. Yan and J. L. Liu, *Dalton Trans.*, 2011, **40**, 4933.

9 (*a*) B. Yan and X. F. Qiao, *J. Phys. Chem. B*, 2007, **111**, 12362; (*b*) X. F. Qiao and B. Yan, *J. Phys. Chem. B*, 2008, **112**, 14742; (*c*) X. F. Qiao and B. Yan, *Inorg. Chem.*, 2009, **48**, 4714; (*d*) X. F. Qiao and B. Yan, *Dalton Trans.*, 2009, **38**, 8509.

10 (*a*) X. F. Qiao and B. Yan, *J. Phys. Chem. B*, 2009, **113**, 11865; (*b*) B. Yan, L. M. Zhao, X. L. Wang and Y. Zhao, *RSC Adv.*, 2011, **1**, 1064. (*c*) D. M. Wang. J. H. Zhang, Q. Lin, L. S. Fu, H. J. Zhang and B. Yang, *J. Mater. Chem.*, 2003, **13**, 2279; (d*)* X. F. Qiao and B. Yan, *New J. Chem.*, 2011, **35**, 568.

11 (*a*) J. Feng, S. Y. Song, W. Q. Fan, L. N. Sun, X. M. Guo, C. Y. Peng, J. B. Y. N. Yu and H. J. Zhang, *Microp. Mesop. Mater.*, 2009, **117**, 278; (*b*) Y. Li and B. Yan, *Microp. Mesop. Mater.*, 2010, **128**, 62; (*c*) Q. G. Meng, P. Boutinaud, A. C. Franville, H. J. Zhang and R. Mahiou, *Microp. Mesop. Mater.*, 2003, **65**, 127.

12 (*a*) L. N. Sun, S. Dang, J. B. Yu, J. Feng, L. Y. Shi and H. J. Zhang *J. Phys. Chem. B*, 2010, **114**, 16393; (*b*) Y. Li, B. Yan and Hong Yang, *J. Phys. Chem. C*, 2008, **112**, 3959; (*c*) Y. Y. Li, B. Yan, L. Guo and Y. J. Li, *Microp. Mesop. Mater.*, 2012, **48**, 73; (*d*) Y. J. Li, B. Yan and L. Wang, *Dalton Trans.*, 2011, **40**, 6722.

13 (*a*) X. M. Guo, H. D. Guo, L. S. Fu, R. P. Deng, W. Chen, J. Feng, S. Dang and H. J. Zhang, *J. Phys. Chem. C*, 2009, **113**, 2603; (*b*) Y. Li, B. Yan and Y. J. Li, *Microp. Mesop. Mater.*, 2010, **132**, 87; (*c*) Y. J. Li, L. Wang and B. Yan, *J. Mater. Chem*., 2011, **21**, 1130.

14 (*a*) Y. Zhao and B. Yan, *Dalton Trans.*, 2012, **41**, 5334; (*b*) Y. Zhao and B. Yan, *J. Coll. Interface Sci.*, 2013, **395**, 145; (*c*) Q. P. Li and B. Yan, *RSC Adv.*, 2012, **2**, 10840.

15 (*a*) J. Cuan and B. Yan, *Dalton Trans.*, 2013, **42**, 14230; (*b*) J. Cuan and B. Yan, *RSC Adv.*, 2013, **3**, 20077; (*c*) J. Cuan and B. Yan, *Microp. Mesop. Mater.*, 2014, **183**, 9; (*d*) J. Cuan and B. Yan, *RSC Adv*., 2014, **4**, 1735.

16 (*a*) Y. G. Wang, H. R. Li, J. J. Gu, Q. Y. Gan, Y. N. Li and G. Calzaferri, *Microp. Mesop. Mater.*, 2009, **121**, 1; (*b*) P. P. Cao, Y. G. Wang, H. R. Li and X. Y. Yu, *J. Mater. Chem.*, 2011, **21**, 2709; (*c*) J. N. Hao and B. Yan, *Dalton Trans.*, 2014, **43**, 2810.

17 (*a*) S. L. James, *Chem. Soc. Rev.*, 2003, **32**, 276; (*b*) M. Kurmoo, *Chem. Soc. Rev.*, 2009, **38**, 135; (*c*) S. Natarajan and P. Mahata, *Chem. Soc. Rev.*, 2009, **38**, 2304.

18 (*a*) M. D. Allendorf, C. A. Bauer, R. K. Bhakta and R. J. T. Houk, *Chem. Soc. Rev.*, 2009, **38**, 1330; (*b*) J. Rocha, L. D. Carlos, F. A. Almeida Paz and D. Ananias, *Chem. Soc. Rev.*, 2011, **40** , 926; (*c*) Y. J. Cui, Y. F. Yue, G. D. Qian and B. L. Chen, *Chem. Rev.*, 2012, **112**, 1126; (*d*) L. E. Kreno, K. Leong, O. K. Farha, M. Allendorf, R. P. Van Duyne and J. T. Hupp, *Chem. Rev.*, 2012, **112**, 1105.

19 (*a*) Z. Q. Wang and S. M. Cohen, *Chem. Soc. Rev.*, 2009, **38**, 1315; (*b*) V. Valtchev, G. Majano, S. Mintova and J. Perez-Ramırez, *Chem. Soc. Rev.*, 2013, **42**, 263.

20 (*a*) B. Reimer, B. Gil, B. Marszalek and N. Stock, *CrystEngComm*, 2012, **14**, 4119; (*b*) Y. Zhou and B. Yan, *Inorg. Chem.*, 2014, **53**, 3456.

21 (*a*) P. Liu, H. R. Li, Y. G. Wang, B. Y. Liu, W. J. Zhang, Y. J. Wang W. D. Yan, H. J. Zhang and U. Schubert, *J. Mater. Chem.*, 2008, **18**, 735; (*b*) L. Guo, L. S. Fu, R. A. S. Ferreira, L. D. Carlos, Q. P. Li and B. Yan, *J. Mater. Chem.*, 2011, **21**, 15600.

22 (*a*) J. Cuan and B. Yan, *RSC Adv.*, 2014, **4**, 1735; (*b*) Z. Y. Yan and B. Yan, *New J. Chem.*, 2014, **DOI:** 10.1039/C3NJ01639K.

23 J. G. DeShazer and G. H. Dieke, *J. Chem. Phys.*, 1963, **38**, 2190.